

Ex vivo rheology of spider silk

N. Kojić^{1,2}, J. Bico¹, C. Clasen³ & G.H. McKinley¹

¹*Hatsopoulos Microfluids Laboratory, Department of Mechanical Engineering, MIT,*

²*Harvard-MIT Division of Health Sciences and Technology,*

Cambridge, Massachusetts 02139, USA.

³*Institut für Technische und Macromolekulare Chemie, 20146 Hamburg, Germany.*

Submitted to *Nature Materials*; May 7, 2003

The spinning process developed by spiders over millions of years provides a great example of a natural microfluidic system and remains a considerable source of questions¹⁻³. In order to probe the rheological properties of minute amounts of the spinning material extracted *ex vivo* from the major ampullate gland of a *Nephila clavipes* spider we have developed two new micro-rheometric devices⁴⁻⁶. The present study shows that the spinning liquid is a complex viscoelastic fluid. Its shear viscosity (resistance to flow) decreases ten-fold as it is pushed through the narrow spinning canals of the spider, whereas its extensional viscosity (resistance to stretching) increases more than one hundred-fold during the spinning process. Quantifying the properties of native spinning solutions provides new guidance for adjusting the spinning processes of synthetic or genetically-engineered silks to match those of the spider.

During the past decade spider dragline silk has been revered for having unmatched mechanical properties⁷⁻⁹, yet how exactly the spider makes its fibre remains unclear. Recent experiments with recombinant spider silk³ and other studies performed with silkworms⁷ show that careful control of the processing conditions for fibre spinning is key to obtaining superior mechanical properties in spun silks. To understand this complex flow process it is essential to elucidate the rheological properties of the initial spinning material (commonly

referred to as “spinning dope”¹) that is stored in the spinning glands of the spider. Although the spinning dope is a concentrated aqueous solution containing 25-30 wt.% protein (mainly Spidroin), all rheological experiments to date have been performed with diluted solutions (<5 wt.%)¹⁰. These experiments suggest non-Newtonian fluid properties, however more insight would be gained through direct rheological characterisation of the native, concentrated dope. The majority of micro-rheometric techniques available for the characterization of complex biofluids rely on Brownian forcing of microscopic tracer beads and the rheological properties of the surrounding fluid matrix are then deconvolved from the time-correlated displacement of the bead¹¹. Such techniques are inherently limited to studies of linear viscoelastic properties of the test fluid at small shearing strains. By contrast, the silk spinning process involves large strains and both shearing and extensional kinematic components. To address these concerns, two new micro-rheometric instruments have been constructed: a flexure-based micro-rheometer for steady and oscillatory shearing measurements and a capillary breakup micro-rheometer for extensional rheometry⁴⁻⁶. Both of the experimental devices were specifically designed to accommodate the small quantities (~1–5 μ L) of fluid available from each of the major ampullate glands of a single *Nephila clavipes* ‘golden orb weaving’ spider (Fig. 1). Thus, these micro-rheometric devices enable *ex vivo* testing of the spinning dope from which the spider spins dragline and web frame fibres⁸.

The micro-rheometer⁴ generates a plane Couette shearing flow between two optical flat plates aligned using white light interferometry and separated by a precisely-controlled gap of 1–200 μ m (Fig. 2a). The shear stress exerted on the sample (ranging from 2 to 10⁴ Pa) is calculated from the deflection of the upper flexure as the lower one is actuated. The imposed shear rate, defined as the ratio of the actuated plate velocity and the inter-plate gap, $\dot{\gamma} = V/h$, can be varied over the range $2 \times 10^{-4} < \dot{\gamma} < 4 \times 10^2 \text{ s}^{-1}$. The micro-rheometer was

used to measure the shear-rate-dependence of the steady shear viscosity $\eta(\dot{\gamma})$ for a 1 μL blob of spinning dope extracted from the major ampullate gland. The dope was sheared between two 25 mm² optical plates with the gap set to 25 μm (Fig. 2a). In the limit of zero shear rate, the data in Figure 2(b) shows that the viscosity of the spinning dope is $\eta_0 = 3500 \text{ Pa}\cdot\text{s}$ (or 3.5×10^6 times the viscosity of water). However, under stronger deformation rates the dope viscosity drops significantly with increasing shear rate, i.e. the dope shear thins (Fig. 2b). This effect is characteristic of concentrated polymer solutions due to the loss of molecular entanglements and can be described by molecular theories or by phenomenological constitutive models such as the Carreau-Yasuda equation^{12,13}:

$$\eta = \eta_0 [1 + (\dot{\gamma}\lambda)^a]^{(n-1)/a}, \quad (1)$$

where λ is a measure of the relaxation time of the viscoelastic fluid (its inverse is the critical shear rate that marks the onset of shear thinning), n is the power-law exponent characterizing the shear-thinning regime observed at high shear rates, and the coefficient a describes the transition between the zero-shear-rate region and the power-law region. Nonlinear regression of these parameters to our data yields values of $\lambda = 0.40 \text{ s}$, $a = 0.68$ and $n = 0.18$, which are characteristic for a shear-thinning fluid¹².

During a typical spinning process^{1,7}, the *Nephila* spider draws out a 4 μm diameter thread at a speed of 20 mm/s corresponding to a flow rate of $Q = 0.25 \text{ nL/s}$. We approximate the geometry of the long converging spinning canal (or *S-duct*) shown in Figure 1(b) as a truncated cone of length $L = 20 \text{ mm}$, and with maximum/minimum diameters of $D = 200 \mu\text{m}$ and $d = 4 \mu\text{m}$ respectively. For the given geometry and flow rate, the pressure drop required to push the viscous dope through the canal can be estimated

from hydrodynamic lubrication theory, which gives the following relation for the flow of a power-law liquid through a tapered tube¹³:

$$\Delta P = \frac{2^{3n+2}\eta_0\lambda^{n-1}L}{3n} \left[\frac{Q}{\pi} \left(\frac{1}{n} + 3 \right) \right]^n \left(\frac{d^{-3n} - D^{-3n}}{D - d} \right), \quad (2)$$

Here η_0 , λ and n are obtained from the Carreau-Yasuda model (1). This relation is only valid in the shear-thinning regime when the shear rate is larger than the critical shear rate ($1/\lambda$). For our truncated cone geometry, the minimum value of the wall shear rate is $\dot{\gamma} = 32Q/\pi D^3 = 0.3\text{s}^{-1}$, which justifies the use of the power law fluid and equation 2 as an approximation. The pressure drop thus computed is $\Delta P = 3.8 \times 10^7$ Pa which is a factor of 500 lower than the value (1.9×10^{10} Pa) expected from the corresponding Newtonian calculation (corresponding to setting $n = 1$ in equation 2). However the computed value of ca. 380 atm. still exceeds reasonable physiological limits for a spider. Although shear thinning alone does not appear to decrease the total pressure drop sufficiently, it can act synergistically with other proposed mechanisms such as a shear-induced transition to a liquid crystalline phase¹, localised slip of the polymer solution on the tube wall¹⁴, or a subtle form of lubrication, such as a watery surfactant layer¹ or an analogue to the sericin coat surrounding fibroin fibres spun by the silkworm *Bombyx mori*².

In addition to being sheared, the viscoelastic spinning solution is also stretched due to the elongational flow experienced in the converging duct and the subsequent spinline. An extensional flow of this type is characterized by two parameters¹³; the deformation rate and the total Hencky strain accumulated, which can be defined in the present problem as $\varepsilon = 2\ln(D/d) \approx 8$. This large value of the extensional strain suggests that the Spidroin chains are being considerably extended¹⁵. This extension thus plays a key role in the molecular alignment necessary for the exceptional mechanical properties of the spun fibre. The

characteristic strain rate for this elongational flow is given by $\dot{\epsilon} = \frac{4Q}{\pi L} \left(\frac{1}{d^2} - \frac{1}{D^2} \right) = 1 s^{-1}$. This rate of stretching can be compared with the liquid relaxation time via the Deborah number¹³ (defined as $De = \lambda \dot{\epsilon}$) which provides a dimensionless measure of the importance of viscoelastic properties. The computed value of $De \approx 0.5$ indicates that viscoelastic effects should result in strain hardening of the dope (i.e. an increase in the resistance to stretching with increasing strain)¹³. This strain-hardening effect is due to chain-stretching of the entangled Spidroin macromolecules and the presence of this additional elastic stress can be evaluated from the ‘extensional viscosity’ of the liquid. If macroscopic volumes of the entangled polymer solution are available then this extensional viscosity can be measured using a filament stretching rheometer¹⁶. However, given the limited amount of raw dope available this method becomes impractical, and thus we have developed a microscale capillary break-up extensional rheometer to measure the transient extensional viscosity η_e ^{5,6}. The experimental procedure involves placing 1 μ L of the spinning dope in between two cylindrical endplates separated by an initial gap of 1 mm to form a liquid bridge. The plates are then pulled apart to a distance of 5 mm in order to impose a step axial strain on the sample and form a liquid thread (Fig. 3). The viscoelastic column thins under the action of capillarity, while viscous and elastic forces tend to impede the necking process. Thus, the extensional viscosity can be deduced from the self-similar thinning and pinch-off dynamics of the viscous fluid thread⁶:

$$\eta_e = \frac{0.426(\sigma/R)}{-\frac{2}{R} \frac{dR}{dt}} = -\frac{0.213\sigma}{dR/dt}, \quad (3)$$

where σ is the surface tension of the liquid (estimated to be approximately 70 mN/m, as for water), $R(t)$ is the midpoint radius of the thread (measured with a laser micrometer), and the prefactor is derived from a slender-body theory in order to account for deviations from a

purely cylindrical geometry in the vicinity of the endplates⁶. The data in Figure 3 shows that at small strains η_e is three times larger than the zero-shear-rate viscosity measured with the shearing micro-rheometer (this observation is consistent with the classical results of Trouton for a Newtonian liquid¹⁷). However, at large strains the necking dynamics are greatly retarded as the filament simultaneously strain hardens and undergoes mass transfer to the surroundings (i.e. drying). This strain-hardening stabilizes the spinline and leads to the formation of axially-uniform filaments¹⁸.

Orb-weaving spiders have evolved a specialized fibre-spinning process that exploits the nonlinear rheology of a complex fluid. In the spinning canal of *Nephila clavipes*, the shear viscosity of the spinning dope decreases by an order of magnitude in order to reduce the required driving pressure, whereas the extensional viscosity increases by a factor of 100 to stabilise the fluid thread and inhibit capillary break-up of the spun thread. Tailoring the rheological properties of artificial dopes containing genetically modified or reconstituted silks to match the *ex vivo* properties of the natural dope may prove essential in enabling us to successfully process novel synthetic materials with mechanical properties comparable to, or better than, those of natural spider silk.

Acknowledgements: This research is supported by funds from the NASA Biologically-Inspired Technology Program, the DuPont-MIT Alliance and by the MIT Institute for Soldier Nanotechnology (ISN). The authors would like to acknowledge Rachél Rogers from the Miami Metrozoo, Florida, for generously providing *N. Clavipes* specimens.

References

1. Vollrath, F. & Knight, D. P. Liquid crystalline spinning of spider silk. *Nature* **410**, 541–548 (2001).
2. Kaplan, D. L., Adams, W. W., Viney, C. & Farmer, B. L. *Silk Polymers: Materials Science and Biotechnology* (ACS, Washington, 1994).
3. Lazaris, A., *et al.* Spider silk fibers spun from soluble recombinant silk produced in mammalian cells. *Science* **295**, 472–476 (2002).
4. Gearing, B.P. & Anand, L. A novel testing apparatus for tribological studies at the small scale. *Proc. 2001 ASME Int. Mech. Eng. Congress and Exposition*.
5. Bazilevsky, A.V., Entov, V. M. & Rozhkov, Liquid filament microrheometer and some of its applications. *Proc. of the Golden Jubilee meeting of the British Society of Rheology*, Elsevier, (1990).
6. McKinley, G.H. & Tripathi, A., How to extract the Newtonian viscosity from capillary breakup measurements in a filament rheometer. *J. Rheol.*, **44**, 653-670 (2000).
7. Shao, Z., & Vollrath, F. Surprising strength of silkworm silk. *Nature* **418**, 741 (2002).
8. Gosline, J.M., Guerrete P.A., Ortlepp C.S. & Savage K.N., The mechanical design of spider silks: from fibroin sequence to mechanical function. *J. Exp. Biol.* **202**, 3295-3303 (1999).
9. Becker, N. *et al.* Molecular nanosprings in spider capture-silk threads. *Nature Materials* **2**, 278-283 (2003).
10. Chen, X., Knight, D.P. & Vollrath, F. Rheological characterisation of *Nephila* spidroin solution. *Biomacromolecules* **3**, 644-648 (2002).

11. Solomon, M. and Lu, Q., Rheology and Dynamics of Particles in Viscoelastic Media, *Curr. Opin. Colloid & Int. Sci.*, **6**, 430-437, (2001).
12. Yasuda, K., Armstrong, R.C. & Cohen, R.E. Shear-flow properties of concentrated-solutions of linear and star branched polystyrenes. *Rheol. Acta* **20**, 163-178 (1981).
13. Bird, R.B., Armstrong, R.C. & Hassager, O. *Dynamics of Polymeric Liquids: Volume 1 Fluid Mechanics* (Wiley Interscience, New York, 1987).
14. Migler K.B., Hervet H. & Léger L. Slip transition of polymer melt under shear-stress. *Phys. Rev. Lett.* **70**, 287-290 (1993).
15. Perkins, T.T., Smith, D.E. and Chu, S., Single Polymer Dynamics in an Elongational Flow, *Science*, **276**, 2016-2021, (1997).
16. Bhattecharjee PK, Oberhauser JP, McKinley GH, *et al.* Extensional rheometry of entangled solutions. *Macromolecules* **35**, 10131-10148 (2002).
17. Trouton, F.T., On the coefficient of viscous traction and its relation to that of viscosity. *Proc. Roy. Soc. London A* , **77**, 426-440 (1906).
18. Olagunju D.O. A 1-D theory for extensional deformation of a viscoelastic filament under exponential stretching, *J. Non-Newton Fluid Mech.* **87**, 27-46 (1999).

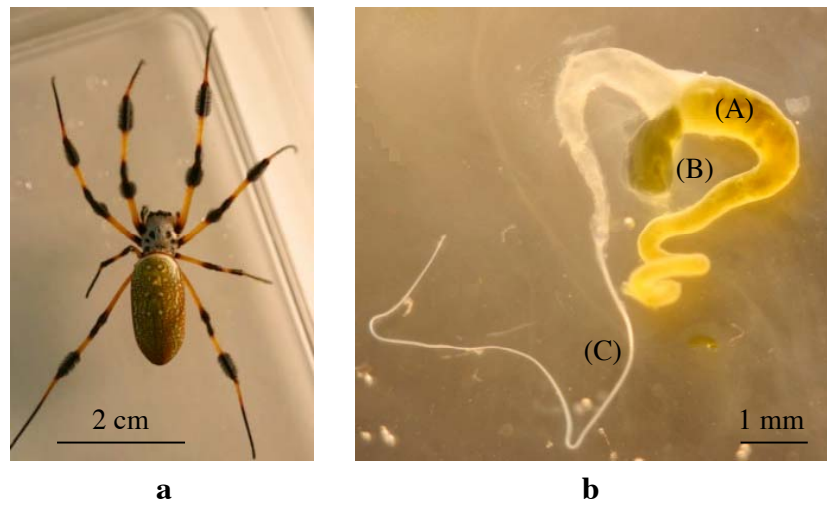


Figure 1: **a**, Adult female *Nephila clavipes* (golden-orb) spider provided by the Miami Metrozoo, Florida. Scale bar is 2cm. **b**, (A) Major Ampullate (MA) gland of the spider (scale bar 1 mm). The 1 μ L blob (B) protruding through a rupture of the gland wall near the spinning canal (C) was used for the rheology experiments.

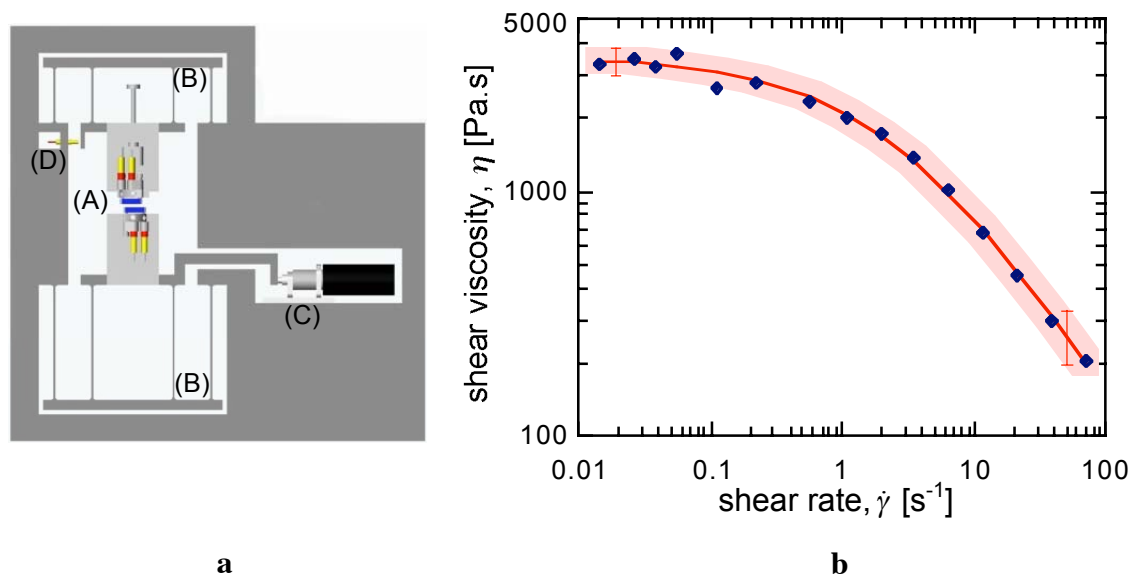


Figure 2: **a**, Schematic diagram of the flexure-based micro-rheometer. The fluid sample is sheared between two interferometrically-aligned flat plates (A). The compound flexure system (B) is actuated by an “inchworm” motor (C) and provides a planar (Couette) shear flow. The shear stress is deduced from the corresponding deflection of the top fixture as detected by an inductive sensor (D). **b**, Shear viscosity of the native silk dope. The solid line represents the Carreau-Yasuda fit from equation (1) to experimental data (markers). Reproducibility was confirmed by testing specimens from two other spiders whose abdomens were similar in size. The variation in the data is represented by the shaded band and corresponds to the standard error bars shown.

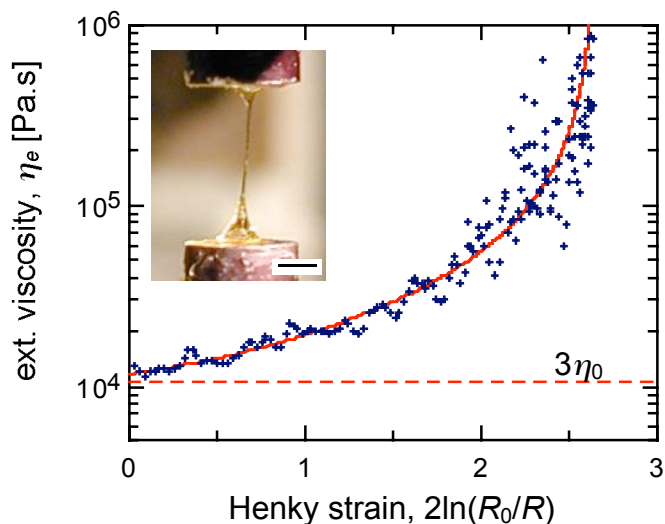


Figure 3: The transient extensional rheology of *ex vivo* silk dope. The extensional viscosity is shown as a function of the total strain in the material. Here, R_0 is the initial diameter of the thread measured at the midpoint between the plates with a laser micrometer. The decrease of the midpoint diameter was monitored over time. The extensional viscosity was then deduced from equation (2) and is represented by the markers. The solid line is an analytical fit of these values. For low strains, we obtain the limit $\eta_e \approx 3\eta_0 = 11400 \text{ Pa}\cdot\text{s}$ as expected for a Newtonian liquid¹⁷ (dashed line). Inset, a silk thread of diameter $60 \mu\text{m}$ formed by separating the plates to a distance of 5 mm and allowing the thread to neck under the action of capillarity and viscoelastic stresses (scale bar is 1 mm).